Journal of Statistical Physics, Vol. 73, Nos. 1/2, 1993

Boundary Critical Behavior of $d=2$ Self-Avoiding Walks on Correlated and Uncorrelated Vacancies

Attilio L. Stella,[1] Flavio Seno,[2] and Carlo Vanderzande[3]

Received February 17, 1993

In this paper we present exact results for the critical exponents of interacting self-avoiding walks with ends at a linear boundary. Effective interactions are mediated by vacancies, correlated and uncorrelated, on the dual lattice. By choosing different boundary conditions, several ordinary and special regimes can be described in terms of clusters geometry and of critical and low-temperature properties of the $\mathcal{O}(n=1)$ model. In particular, the problem of boundary exponents at the Θ'-point is fully solved, and implications for Θ-point universality are discussed. The surface crossover exponent at the special transition of noninteracting self-avoiding walks is also interpreted in terms of percolation dimensions.

KEY WORDS: Surface critical phenomena; multicritical points; Θ-point.

1. INTRODUCTION

Surface critical phenomena have been extensively studied in recent years.[1] For systems with two bulk dimensions, the critical behavior at boundaries is interesting mainly for theoretical reasons, but may be also particularly important in the discussion of difficult universality issues. An example of this, directly connected with the results presented here, is the controversy over the universality of the so-called Θ- and Θ'-points for models of linear polymers.[2–19],[4]

[1] Dipartimento di Fisica and Sezione INFN, Bologna, Italy.
[2] Theoretical Physics, Oxford University, Oxford, U.K.
[3] Limburgs Universitarium Centrum, Diepenbeek, Belgium.
[4] The connection between the Θ-like point found in ref. 17 and the Θ'-point is discussed in ref. 35.

0022-4715/93/1000-0021$07.00/0

A linear polymer in the presence of a wall can be modeled by a self-avoiding walk (SAW) on a semi-infinite lattice. The linear boundary represents the wall. Suitable interaction energies can be attributed to contacts of the SAW with the boundary and to close approaches of nonconsecutive walk sites (monomers) along the chain.

Upon increasing the energy of adsorption on the wall, the polymer undergoes the so-called special transition, which separates the ordinary, desorbed critical regime from the adsorbed one.[20,21] Monomer–monomer attraction energies can determine the Θ-collapse transition,[22,23] in which the polymer passes from a swollen, coil structure, with nontrivial fractal properties, to a compact, globular one.

Substantial progress in the field of surface critical behavior in two dimensions has been made on the basis of conformal invariance.[24,25] In particular, for self-avoiding walks, this approach allowed the conjecture of exact values for several boundary exponents.[25,21] As an example, which will concern us here, the presence of an attraction between walk and boundary was studied, leading to exact results for the SAW special surface critical regime.[21] However, conformal invariance has so far only been successfully applied to SAW problems without self-interaction. This excludes intriguing situations, like that occurring when both monomer–boundary and monomer–monomer interactions are present, which can result in interesting multicritical phenomena, such as the special Θ-point, at which adsorption and collapse occur simultaneously.[15]

The introduction of models with percolation vacancies was an important breakthrough in the study of bulk properties of self-attracting SAW, which for the first time allowed an exact determination of critical exponents at the so-called Θ'-point.[2,3] The basic idea of this method,[3] which elaborated on an earlier proposal by Coniglio *et al.*,[2] was to use annealed vacancies as mediators of effective interactions in a SAW problem. Under suitable conditions, one can then establish an identity between SAW and cluster hull statistics, which leads to a determination of bulk exponents, e.g., by connecting them to those of the $\mathcal{O}(n)$ model with $n = 1$. A main goal of this work will be to show the power of the vacancy approach to surface critical phenomena of the Θ'-point and other models.

In ref. 3, a prediction of the entropic surface exponent at the Θ'-point was also attempted by exploiting previous results for the $\mathcal{O}(n)$ model with boundary.[26] This prediction was the cause of a long-standing controversy, since numerical work always failed to confirm it in more standard models.[7,15] This gave rise to a conjecture of nonuniversality for different Θ-point models as a possible explanation of the discrepancy.

A step forward in the understanding of surface critical behavior at the Θ'-point was recently made in ref. 16, where the present authors showed

that the value of the ordinary entropic surface exponent of ref. 3 should instead be attributed to the special one. This progress followed from the first detailed study of the effects of boundary conditions on a SAW model with percolation vacancies, and eliminated a major source of controversy over Θ-point universality.

In the present paper we develop further these ideas and methods and provide for the first time an exact determination also of the ordinary entropic surface exponent at the Θ'-point. This step makes our knowledge of the Θ'-point complete. Further interesting results can be obtained when there is a correlation between the vacancies. In a previous work[27] the present authors showed that it is possible to determine exactly the bulk exponents in the presence of correlated (Ising) percolation vacancies. This allowed us to identify a new universality class of multicritical behavior for interacting SAW in $d=2$.

Here we discuss in detail the SAW surface behavior at this multicritical point following lines similar to those of the uncorrelated case. When correlated vacancies are present, there is a richer variety of boundary conditions one can impose on both walks and vacancies. Correspondingly, two distinct ordinary and one special regime can be exactly characterized, through an identification with Ising model exponents.

This paper is organized as follows: in Section 2 we review briefly the Θ'-point model of refs. 3 and 16 and discuss fully its surface critical regimes, in particular the ordinary one. Section 3 is devoted to the case of SAW on correlated vacancies. In Section 4, on the basis of the vacancy concept, we discuss also the relevance of percolation geometry to the special surface crossover behavior of noninteracting SAW in $d=2$. Section 5 is devoted to conclusions.

2. ORDINARY AND SPECIAL SURFACE EXPONENTS AT THE Θ'-POINT

Let us consider a semi-infinite hexagonal lattice, as sketched in Fig. 1. Each hexagon is occupied or vacant with probability p, or $1-p$, respectively. This specifies a percolation problem on the semi-infinite, dual triangular lattice. For this percolation problem we choose open boundary conditions, i.e., the hexagons touching the border are also occupied with the bulk probability p.

For each percolative configuration C, with probability $P(C)$, we separately consider SAW of two types. In the first case (a) the walk is never allowed to step on the edges of an occupied hexagon. In the second (b) edges of vacant hexagons can never be visited.

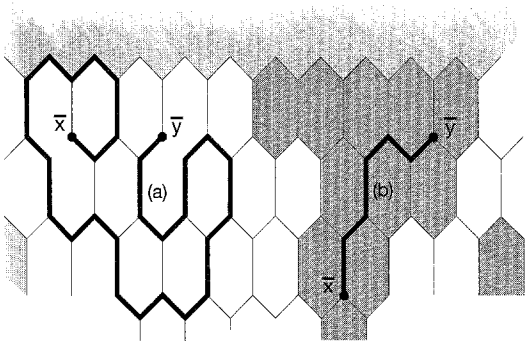

Fig. 1. Occupied (shaded) and vacant (white) hexagons in a given configuration. Examples of type (a) and type (b) walks are given. The type (a) walk has $N_2 = 4$, $N_3 = 1$. Notice that the type (b) walk cannot step on the boundary.

The grand canonical generating function of the SAW problem is, in both cases, of the form

$$Z(K, p) = \sum_C P(C) \sum_{\{W\}_C} K^{|W|} \tag{2.1}$$

where $\{W\}_C$ indicates the set of SAW, W, compatible with C, with $|W|$ steps, and, for example, one end at a given origin O. Alternatively we can replace W by a self-avoiding ring $\mathscr{R}$. Here K is the step fugacity and the p dependence comes through $P(C)$. By performing the summation over C first, the generating function becomes

$$Z(K, p) = \sum_W \rho(p)^{H(W)} K^{|W|} \tag{2.2}$$

where now the sum is over all SAW and $\rho(p) = 1 - p$, or p in cases (a) and (b), respectively. $H(W)$ represents the number of distinct lattice hexagons whose edges are visited by W.

It is easy to check[3] that, for an open walk which never touches the border,

$$H = |W| + 1 - N_2(W) - 2N_3(W) \tag{2.3}$$

where N_2 and N_3 are the numbers of hexagons visited, not consecutively, 2 and 3 times, respectively, by steps of W. So, the effect of percolation vacancies is to induce local attractive interactions for the walk, which allow for collapse. In contrast to most common models, here one has not only nearest-neighbor interactions, but also a special subset of next-nearest-neighbor interactions.[2,3] For that reason the collapse point of this model is called the Θ'-point.[2]

As long as one considers walks within the bulk and fixes $p = 1/2$, the percolation threshold on a triangular lattice, there is no difference between cases (a) and (b). Indeed $p = 1/2$ identifies the bulk Θ'-point. As shown in ref. 3, at the Θ'-point one can determine the exponent $\nu_{\Theta'}$ by exploiting the fact that a self-avoiding ring of type (a) or (b) at $K = K_{\Theta'} = 1$ has the same statistics as the hull of percolation clusters. This implies that the grand canonical average radius of gyration of the ring behaves as

$$R(K, p) = \frac{\sum_{\mathscr{R}} K^{|\mathscr{R}|} \rho(p)^{H(\mathscr{R})} R(\mathscr{R})}{\sum_{\mathscr{R}} K^{|\mathscr{R}|} \rho(p)^{H(\mathscr{R})}} \sim (K_{\Theta'} - K)^{-\nu_{\Theta'}}, \qquad K \to K_{\Theta'}^{-} = 1^{-}, \qquad p = \frac{1}{2} \tag{2.4}$$

where $\mathscr{R}$ is a ring with $|\mathscr{R}|$ steps and gyration radius $R(\mathscr{R})$ with respect to the center of mass. For economy of notations the grand canonical average is also indicated by R. Here $\nu_{\Theta'}$ is equal to the reciprocal of $d_H = 7/4$, the hull fractal dimension of percolation clusters.[28]

By considering the asymptotic behavior of the two-point bulk correlation function,

$$\mathscr{G}(\mathbf{x}, \mathbf{y}, K, p) = \sum_{W, \partial W = \mathbf{x}, \mathbf{y}} K^{|W|} \rho(p)^{H(W)} \simeq |\mathbf{x} - \mathbf{y}|^{-\eta_{\Theta'}} \tag{2.5}$$

where ∂W indicates the endpoints of W, when $p = 1/2$, $K = K_{\Theta'}$, and $|\mathbf{x} - \mathbf{y}| \to \infty$, one can also determine $\eta_{\Theta'}$.

Indeed, at $K = 1$ and $p = 1/2$, as discussed below, this correlation function can be identified with $\langle S_{\mathbf{x}} S_{\mathbf{y}} \rangle$ for an Ising model at zero temperature. One concludes that, in view of the existence of long-range order in the Ising model, $\eta_{\Theta'} = 0$.[3] This also implies that $\gamma_{\Theta'} = \nu_{\Theta'}(2 - \eta_{\Theta'}) = 8/7$, where $\gamma_{\Theta'}$ is the bulk entropic exponent for walks with one end fixed.

The above identification follows from the fact that, on the basis of Eq. (2.1), in case (a), for example, $\mathscr{G}$ can be represented diagrammatically as a sum over self-avoiding paths connecting $\mathbf{x}$ to $\mathbf{y}$ on the hexagonal lattice, in the presence of self-avoiding rings (percolation cluster hulls), which are mutually nonintersecting and do not intersect the path. Each diagram of this type (a typical contribution is sketched in Fig. 2) in the sum has the same weight, due to the choice of parameters ($K = K_{\Theta'} = 1$, $p = p_c = 1/2$).

Now consider an Ising model on a hexagonal lattice with reduced Hamiltonian $K_{\text{Ising}} \sum_{\langle \mathbf{xy} \rangle} S_{\mathbf{x}} S_{\mathbf{y}}$, the sum being restricted to nearest neighbors. An expression of $\langle S_{\mathbf{x}} S_{\mathbf{y}} \rangle$ in term of high-temperature diagrams clearly produces the same sum as that in $\mathscr{G}$ when $\tanh(K_{\text{Ising}}) = 1$, i.e., at zero temperature.

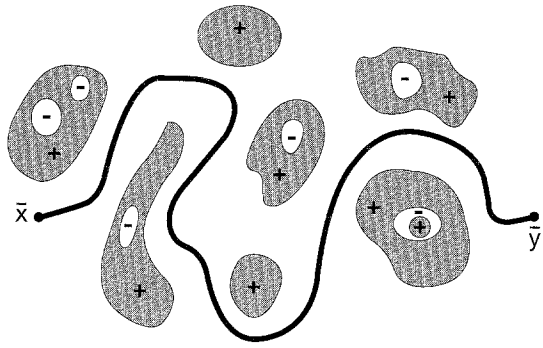

Fig. 2. Schematic representation of a contribution to $\mathscr{G}$ in the bulk. The heavy line joining x to y represents a self-avoiding path on the lattice, all contained in a − region. The rings correspond to hulls separating vacant (−) from occupied (+) hexagons.

We now turn to a determination of surface critical exponents at the Θ'-point. To this purpose we consider rings of type (a) which have to pass through a given point O of the boundary. It is easy to check that $H(\mathscr{R})$ for such a ring becomes[16]

$$H(\mathscr{R}) = |\mathscr{R}| - N_2(\mathscr{R}) - 2N_3(\mathscr{R}) - N_b(\mathscr{R}) \tag{2.6}$$

where $N_b(\mathscr{R})$ is the number of points of the border belonging both to $\mathscr{R}$ and to separation edges between hexagons in the last upper row (see Fig. 3). This last result indicates that the boundary exerts an effective attraction on the ring, since configurations with higher N_b are favored. For a ring experiencing attractive interactions with itself and with a boundary we would expect the possibility of both a bulk Θ transition and a surface adsorption special transition.[1] If we generalize the model in Eqs. (2.1)–(2.2) by making the replacements

$$\begin{aligned} K^{|\mathscr{R}|}(1-p)^{|\mathscr{R}|} &\to K'^{|\mathscr{R}|} \\ (1-p)^{-N_2(\mathscr{R})-2N_3(\mathscr{R})} &\to \exp \omega[N_2(\mathscr{R}) + 2N_3(\mathscr{R})] \\ (1-p)^{-N_b(\mathscr{R})} &\to \exp[\omega_s N_b(\mathscr{R})] \end{aligned} \tag{2.7}$$

with ω and ω_s having the meaning of independent reduced attraction and adsorption energies, respectively, the above transitions are expected to be marked by multicritical lines in the (ω, ω_s) plane (Fig. 4). At all points below the adsorption line, the surface critical behavior is ordinary. For example, a ring attached to the boundary by one end, asymptotically, has on average a vanishing fraction of steps on the boundary. Above the same line this fraction is asymptotically nonzero.

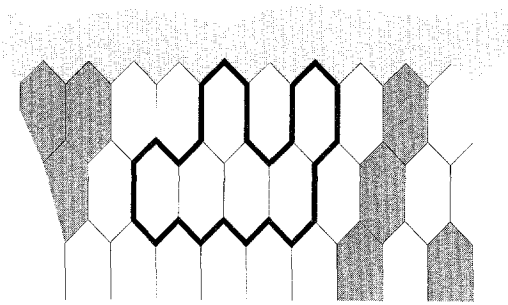

Fig. 3. Type (a) self-avoiding ring, with $N_2=3$, $N_3=0$, and $N_b=4$.

If we consider

$$\langle N_b \rangle = \frac{\partial}{\partial \omega_s} \log Z \tag{2.8}$$

with

$$Z = \sum_{\mathscr{R}} K'^{|\mathscr{R}|} \exp\{\omega[N_2(\mathscr{R}) + 2N_3(\mathscr{R})]\} \exp[\omega_s N_b(\mathscr{R})] \tag{2.9}$$

we expect that

$$\langle N_b \rangle \sim [K'_C(\omega) - K']^0 \sim \text{const} \qquad \text{for} \quad K' \to K'_C(\omega)^- \tag{2.10}$$

and

$$\langle N_b \rangle \sim [K'_C(\omega, \omega_s) - K']^{-1} \qquad \text{for} \quad K' \to K'_C(\omega, \omega_s)^- \tag{2.11}$$

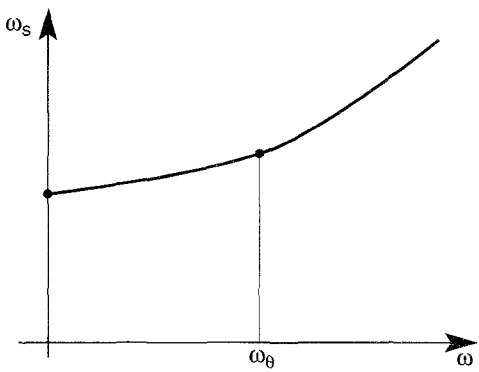

Fig. 4. Qualitative diagram for different critical regimes of a SAW rooted on the boundary and subject to self-attraction (ω) and adsorption (ω_s). The vertical segment separates swollen from collapsed situations, while the other line marks the transition from ordinary (lower region) to adsorbed (upper region) regimes. The special Θ-point is marked by a heavy dot.

for the ordinary and adsorbed regimes, respectively. For (ω, ω_s) on the adsorption special line, one expects

$$\langle N_b \rangle \sim [K'_C(\omega) - K']^{-\phi_s} \qquad \text{for} \quad K' \to K'_C(\omega)^- \tag{2.12}$$

where $0 \leqslant \phi_s \leqslant 1$ is the surface crossover exponent. In Eqs. (2.10), (2.12), we have taken into account that the critical step fugacity K'_C does not depend on ω_s for ordinary and special regimes. In all cases

$$\langle |\mathscr{R}| \rangle \sim (K'_C - K')^{-1} \qquad \text{for} \quad K' \to K'^-_C \tag{2.13}$$

By considering that in each ring configuration

$$\frac{N_b - 1}{2} \leqslant N_s \leqslant N_b \tag{2.14}$$

with N_s representing the number of steps on the boundary, we conclude that the behaviors (2.10)–(2.12) apply also to $\langle N_s \rangle$.

Fixing $p = 1/2$, we can see from Fig. 4 that our model (2.4) is clearly on the vertical theta line as far as bulk properties are concerned.

The question is to decide which surface regime applies to a ring passing through a point on the boundary. With the boundary conditions of type (a) specified above, the ring is statistically indistinguishable from the contour of a cluster in the percolation problem on a semi-infinite triangular lattice. If we consider $\langle N_s \rangle$ for ring configurations passing through O, we obtain the same result as when considering the average number of steps on the border for hulls enclosing occupied hexagons and passing through O. In both cases the allowed configurations generated by (2.1) consist of a self-avoiding ring, which is constrained to avoid the remaining hulls in the system. By construction, the statistical weight of any configuration for the ring problem is the same as for the hull case [the weight in Eq. (2.1) is actually the same for all configurations].

From conformal invariance we know that the fractal dimension of the intersection of a percolation cluster with a boundary is equal to 2/3.[25,29]

If we put $K'_{\Theta'} = K'_C(\omega_{\Theta'})$, with $\omega_{\Theta'} = \log 2$, the radius of gyration of the ring must grow like

$$R(K', \omega_{\Theta'}) \sim (K'_{\Theta'} - K')^{-4/7} \qquad \text{for} \quad K' \to K'^-_{\Theta} \tag{2.15}$$

consistent with the hull fractal dimension $d_H = 7/4$. On the other hand we must also have

$$\langle N_s \rangle \sim R^{2/3} \sim (K'_{\Theta'} - K')^{-8/21} \qquad \text{for} \quad K' \to K'^-_{\Theta} \tag{2.16}$$

This equation, compared with (2.12), tells us that the type (a) ring is actually at the special Θ'-point, the point of intersection of the Θ and special lines in Fig. 4. This is indeed the only point on the $\omega = \omega_{\Theta'}$ line at which a behavior of the form (2.12), with $0 < \phi_s < 1$, is expected. We thus conclude that the exact value of the surface crossover exponent at the Θ'-point is $\phi_s = 8/21$. This prediction has also been confirmed by numerical analysis.[16]

In order to determine surface entropic exponents at the special Θ'-point, we consider $\mathscr{G}_1(\mathbf{x}, \mathbf{y}, K, p)$ for a SAW(a), with both $\mathbf{x}$ and $\mathbf{y}$ lying on the boundary. This $\mathscr{G}_1$, at $K = 1$ and $p = 1/2$, coincides with the correlation function of the $T = 0$ Ising model on a semi-infinite hexagonal lattice. Indeed, all diagrams for $\mathscr{G}_1$ are given by a SAW joining $\mathbf{x}$ to $\mathbf{y}$, surrounded by closed self-avoiding rings representing the hulls of the percolation clusters in the given C configuration. All such diagrams (see Fig. 5) have the same weight at $p = 1/2$, $K = K_{\Theta'} = 1$, namely, the probability of the corresponding C configuration. For a $T = 0$ Ising model on a hexagonal lattice, the correlation $\langle S_{\mathbf{x}} S_{\mathbf{y}} \rangle$, up to a normalization, is also given by such diagrams, where to each step of the walk or of the closed rings is attributed a factor $\tanh(K_{\text{Ising}}) = 1$. The normalization in this case is given by the Ising partition function, that is, the sum over all configurations of self- and mutually avoiding rings.

Since at $T = 0$, the $d = 2$ Ising model has long-range order also at a boundary, we have that

$$\langle S_{\mathbf{x}} S_{\mathbf{y}} \rangle \to \text{const} \qquad \text{for} \quad |\mathbf{x} - \mathbf{y}| \to \infty \tag{2.17}$$

Thus, by identification, we must have that

$$\mathscr{G}_1(\mathbf{x}, \mathbf{y}, 1, 1/2) \sim 1/|\mathbf{x} - \mathbf{y}|^{\eta_s} \to \text{const} \tag{2.18}$$

when $\mathbf{x}$ and $\mathbf{y}$ belong to the boundary and $|\mathbf{x} - \mathbf{y}| \to \infty$. Equation (2.18) entails $\eta_s = 0$. By standard scaling we also get $\gamma_{1sp} = \nu_{\Theta'}(2 - \eta_{\Theta'}/2 - \eta_s/2) = 8/7$, γ_{1sp} being the entropic exponents for walks with only one end fixed on the boundary.

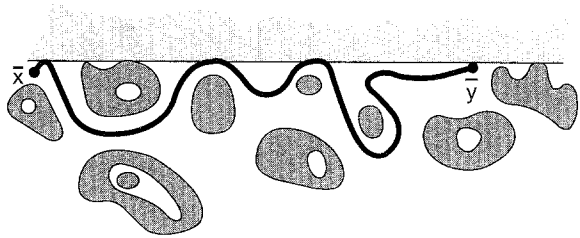

Fig. 5. Typical diagram contributing to $\mathscr{G}_1$ for type (a) walks.

This completes the determination of special Θ'-point surface exponents, as already reported in ref. 16.

The problem of ordinary Θ'-point surface behavior is solved below.

When considering a SAW of type (b) in the presence of the boundary, we immediately realize that their statistical properties must be different from those of type (a) even if $p = 1/2$. Due to the different constraints, type (b) walks can never step on the border. Indeed they have to develop within fully occupied regions. Actually, by comparison with case (a) we argue that the border is not exercising an attractive action now, but rather a repulsion, on the walk. With reference to Fig. 4, this means that the point $p = 1/2$, $K = 1$ for type (b) SAW attached to the border should fall somewhere in the interior of the vertical segment of ordinary Θ'-point surface transitions.

In order to predict the correct η_s for a type (b) SAW, we consider the diagrams contributing to $\mathscr{G}_1$ with $\mathbf{x}$ and $\mathbf{y}$ both fixed close to the boundary, for example within one lattice spacing from it, as sketched in Fig. 6.

With reference to Eqs. (2.1) and (2.5), it is clear that in each configuration C from which nonzero contributions to $\mathscr{G}_1$ arise, there must be an occupied cluster whose hull encloses both $\mathbf{x}$ and $\mathbf{y}$, together with the connecting self-avoiding path (Fig. 6). If the chosen distance of both $\mathbf{x}$ and $\mathbf{y}$ from the boundary were larger, there would of course be more than a single hull enclosing both $\mathbf{x}$ and $\mathbf{y}$, but their number would still be odd (see below).

In order to discuss $\mathscr{G}_1$ in this case we have to rely on results for the so-called watermelon correlation functions of the $\mathcal{O}(n)$ model. In the geometrical loop version of this model, watermelon correlations with L legs are defined as

$$G_L(\mathbf{x}, \mathbf{y}, M) = \sum_{\mathscr{C}_L(\mathbf{x},\mathbf{y})} W(\mathscr{C}_L) \Big/ \mathscr{Z}_{\mathcal{O}(n)} \tag{2.19}$$

where $\mathscr{C}_L$ represents all diagrams with L self-avoiding paths joining points "at" $\mathbf{x}$ and $\mathbf{y}$, in the presence of self-avoiding loops. Loops and paths are also mutually avoiding, of course. The weight for each such configuration

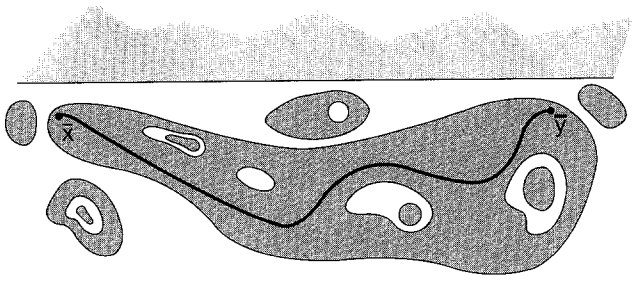

Fig. 6. Typical diagram contributing to $\mathscr{G}_1$ for type (b) walks.

is $W(\mathscr{C}_L) = M^{N_b} n^{N_l}$, where N_b and N_l are, respectively, the total numbers of hexagonal bonds and of closed loops in $\mathscr{C}_L$, and M is a step fugacity. Diagrams contributing to $\mathscr{Z}_{\mathscr{O}(n)}$ are made only of self- and mutually avoiding loops, and are weighted in the same way. Now, when $\mathbf{x}$ and $\mathbf{y}$ are chosen near the boundary of the hexagonal lattice and one puts $M = n = 1$, one concludes that $\mathscr{G}_1(\mathbf{x}, \mathbf{y}, 1, 1/2) \sim G_3(\mathbf{x}, \mathbf{y}, 1)$. Indeed, up to details in the neighborhood of $\mathbf{x}$ and $\mathbf{y}$ the diagrams of $\mathscr{G}_1$ coincide and have the same weight as those of G_3.

Correlation functions of the type (2.19) in the bulk have been studied for spin models in the framework of the Coulomb gas and conformal invariance approaches to $d = 2$ critical behavior.[30–32] On the basis of conformal invariance, refs. 33, 26, and 34 were also able to conjecture the surface η exponents for watermelon correlation functions whose points are on a semi-infinite linear boundary.

By putting, $\eta_s = 2x_s^L$, they predicted

$$G_L(\mathbf{x}, \mathbf{y}) \sim |\mathbf{x} - \mathbf{y}|^{-2x_s^L}$$

with x_s^L given, for the case $n = 1$, by the formula

$$x_s^L = \tfrac{1}{6}L^2 - \tfrac{1}{6}L \tag{2.20}$$

which holds in the low-temperature phase.

The case $L = 3$ is the relevant one for the η_s exponent of $\mathscr{G}_1$ for a type (b) SAW. From (2.20) one obtains $x_s^3 = 1 = \eta_s/2$. This implies that $\gamma_{1o} = \nu(2 - \eta_{\Theta'}/2 - \eta_s/2) = 4/7$.

Going back to the case of a type (a) SAW for a moment, we notice that in such a case $\mathscr{G}_1 \sim G_1$, thus implying that the special $\eta_s = 2x_s^1 = 0$, which is consistent with the conclusion already drawn above, taking into account the low-temperature Ising long-range order.

This value of γ_{1o}, as discussed above, must apply to SAW at the Θ'-point in the ordinary regime, as far as surface behavior is concerned. Indeed, this value turns out to be fully consistent with the numerical results obtained so far for both the standard Θ-point model[7,15,18] and for the Θ'-point model,[16] when attraction effects from the boundary are not effective, or are avoided by considering a particular class of walks.

To conclude this section, we show how the watermelon exponents (2.20) can also be used for an alternative independent determination of ϕ_s.

Imagine including in Z the weighted sum over all (a) self-avoiding rings which touch the boundary at least at one point, no matter which one. If we consider a finite portion of boundary of length L and the corresponding quantity Z_L, it is easy to realize that, at $K = 1$, $p = 1/2$,

$$\frac{1}{Z_L}\frac{1}{L}\frac{\partial^2}{\partial \omega_s^2} Z_L \sim \int_0^L dx\, G_2(O, \mathbf{x}) \qquad \text{for} \quad L \to \infty \tag{2.21}$$

where the integral is along the one-dimensional boundary. The derivative with respect to ω_s in the case of our Θ'-model can be performed by formally attributing a value $p_s \neq p$ to the probability of occupation of boundary hexagons and then performing $\partial/\partial p_s$ at $p_s = p = 1/2$. In Eq. (2.21) G_2 is the $n=1$, $T=0$ watermelon function, in which two self-avoiding paths join nearest-neighbor sites at O to nearest-neighbor sites at $\mathbf{x}$.

Since

$$G_2(O, \mathbf{x}) \sim 1/|\mathbf{x}|^{2x_s^2} \qquad \text{for} \quad |\mathbf{x}| \to \infty \tag{2.22}$$

where, according to (2.20), $x_s^2 = 1/3$, the quantity in Eq. (2.21) grows like $L^{1/3}$ for $L \to \infty$. The quantity on the left of Eq. (2.21) clearly has the dimension $-1+2y_s$ in terms of length, and simple finite-size scaling considerations imply a behavior

$$\lim_{L\to\infty} \frac{1}{L} \frac{\partial^2 \log Z}{\partial \omega_s^2} \sim (K_{\Theta'} - K)^{\nu_{\Theta'}(1-2y_s)} \qquad \text{for} \quad K \to K_{\Theta'}^- \tag{2.23}$$

On the other hand, the above results also imply

$$(1-2y_s)\, \nu_{\Theta'} = \nu_{\Theta'} - 2\phi_s = -\tfrac{1}{3}\nu_{\Theta'} \tag{2.24}$$

which means $y_s = 2/3$ and $\phi_s = 8/21$, as already derived above.

A final remark is in order here concerning the fact that η_s for type (b) SAW is the same as for the watermelon function G_3. It is clear that, if points $\mathbf{x}$ and $\mathbf{y}$ are fixed at a larger distance from the boundary, the contribution of diagrams with an odd number of hulls enclosing $\mathbf{x}$ and $\mathbf{y}$ arises. This means that, together with the contribution of G_3, contributions from watermelon functions $G_5, G_7, \ldots$, should add into the asymptotic behavior of $\mathcal{G}_1$. These higher L functions are, of course, less dominant asymptotically, and thus provide only scaling corrections to $\mathcal{G}_1$.

3. WALKS ON CORRELATED ISING VACANCIES

We now consider a modification of the model in the previous section, where the two possible states of each hexagon are characterized by a spin variable $\sigma = \pm 1$, and these Ising spins interact via nearest-neighbor couplings.

The new problem can be conveniently formulated fully in terms of spin language. We introduce, for each site on the hexagonal lattice, an n-component spin $\mathbf{S} \equiv (S^1, S^2, \ldots, S^n)$, with $\mathbf{S}^2 = n$, and on each site of the dual triangular lattice we put an Ising spin $\sigma = \pm 1$.[5] If nearest-neighbor

[5] In the previous section we indicated by S the spin components of an Ising system on the hexagonal lattice. Here we switch to σ to indicate Ising spins on the dual lattice.

edges on the hexagonal lattice are indicated by l and the extrema of the edge l^*, dual of l, by $i^*(l)$ and $j^*(l)$ (Fig. 7), the Hamiltonian

$$-\beta H(\mathbf{S}, \sigma) = K \sum_l (\mathbf{S} \cdot \mathbf{S})_l \frac{(1 \pm \sigma_{i^*(l)})}{2} \frac{(1 \pm \sigma_{j^*(l)})}{2} + L \sum_{l^*} (\sigma\sigma)_{l^*} \tag{3.1}$$

generates the statistics of (a) and (b) rings in the $n \to 0$ limit if $-$ and $+$ signs are chosen, respectively. In Eq. (3.1), $(\mathbf{S} \cdot \mathbf{S})_l$ and $(\sigma\sigma)_{l^*}$ indicate the products of spins at the extrema of edges l and l^*, respectively. So, in the example in Fig. 7 we have $(\mathbf{S} \cdot \mathbf{S})_l = \sum_{\alpha=1}^{n} S_i^\alpha S_j^\alpha$ and $(\sigma\sigma)_{l^*} = \sigma_{i(l^*)} \sigma_{j(l^*)}$.

If we normalize the trace over $\mathbf{S}$ in such a way that $\mathrm{Tr}_{\mathbf{S}}\, 1 = 1$, for any n, the partition function becomes, to leading orders in n,

$$\begin{aligned} Z &= \mathrm{Tr}_{\mathbf{S}}\, \mathrm{Tr}_\sigma \exp(-\beta H) \\ &= Z_{\mathrm{Ising}}(L) \left\{ 1 + n \frac{K^2}{2} \left\langle \sum_l \frac{(1 \pm \sigma_{i^*})}{2} \frac{(1 \pm \sigma_{j^*})}{2} \right\rangle \right. \\ &\quad \left. + n \sum_{\Sigma, \mathscr{R}} \exp(-2L\,|\Sigma|)\, K^{|\mathscr{R}|} \Big/ \sum_{\Sigma} \exp(-2L\,|\Sigma|) + \mathcal{O}(n^2) \right\} \end{aligned} \tag{3.2}$$

In Eq. (3.2), Z_{Ising} is the partition function of the triangular Ising model with coupling L and N_l is the total number of bonds of the hexagonal lattice. In the last term the sum in both numerator and denominator is over all collections Σ of loops on the hexagonal lattice which are self- and mutually avoiding, with total length $|\Sigma|$.

In the numerator the Σ's are summed simultaneously with a self-avoiding ring $\mathscr{R}$ which also avoids Σ. So, this last term now describes a self-avoiding ring with step fugacity K in the presence of Ising vacancies on the dual lattice. The above derivation shows that the statistics of such a ring is obtained in the limit as n goes to zero from the Hamiltonian (3.1).

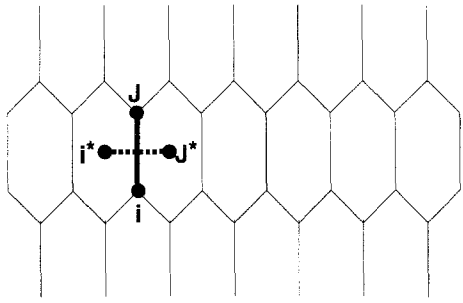

Fig. 7. The heavy edge is a bond l with extrema i and j on the hexagonal lattice. i^* and j^* are the extrema of the dual of l (dotted) on the triangular lattice.

The average radius of gyration of the ring can be written as

$$R=\left\{\sum_{\Sigma}\sum_{\mathscr{R}\text{comp. with }\Sigma} R(\mathscr{R})\left(\prod_{l\in\mathscr{R}} K_l\right)[\exp(-2L)]^{|\Sigma|}\right\} \times\left\{\sum_{\Sigma}\sum_{\mathscr{R}\text{comp. with }\Sigma}\left(\prod_{l\in\mathscr{R}} K_l\right)[\exp(-2L)]^{|\Sigma|}\right\}^{-1} \tag{3.3}$$

where the product over $l\in\mathscr{R}$ contains clearly $|\mathscr{R}|$ terms.

In this product, we indicate by K_b the step fugacity associated to the bond b, which is just K on the basis of Eqs. (3.1) and (3.2). We introduce this more general notation in view of the fact that modifications to the fugacity for steps on the border will be considered below. Notice that when $L=0$, we recover the case of uncorrelated vacancies, described in the previous section. In ref. 27 it has been shown that the ring described by Eq. (3.3) in the bulk is critical at $K=K_c=\exp(-2L_c)$, with L_c representing the critical Ising coupling of the triangular lattice. Furthermore, in these conditions the ring has the same statistics as the hull of Ising clusters. The hull fractal dimension of these clusters has been determined as $d_H=11/8$.[36,28] So, for our ring, $\nu=8/11$.

As discussed below, the bulk η exponent can also be determined by considering

$$\mathscr{G}(\mathbf{x},\mathbf{y},K,L)=\left\{\sum_{\Sigma}\sum_{W\text{comp. with }\Sigma}\left(\prod_{l\in W} K_l\right)[\exp(-2L)]^{|\Sigma|}\right\} \times\left\{\sum_{|\Sigma|}[\exp(-2L)]^{|\Sigma|}\right\}^{-1} \tag{3.4}$$

where the sum in the numerator is again over self-avoiding paths connecting $\mathbf{x}$ to $\mathbf{y}$ and constrained to avoid the hull contours in Σ. For example, for type (a) walks, contributions to this sum can be diagrammatically represented as in Fig. 2, where this time dashed regions correspond to + hexagons, and white regions to − hexagons. In this case, without considering the normalizing denominator, each step l of the SAW from $\mathbf{x}$ to $\mathbf{y}$ implies a factor K_l, while each step of the hulls takes a factor $\exp(-2L)$. By putting $K_l\equiv\exp(-2L_c)$ and $L=L_c$, it is easy to verify that $\mathscr{G}$ becomes the correlation function[6] $\langle S_{\mathbf{x}}S_{\mathbf{y}}\rangle$ for an Ising model on the hexagonal lattice with a coupling K_{Ising}, such that $\tanh(K_{\text{Ising}})=\exp(-2L_c)$. By duality, this Ising model is also critical. Moreover, at $K_l=\exp(-2L_c)$ the

[6] Notice that this Ising model is not the one entering in the Hamiltonian (3.1), which is defined on the dual, triangular lattice.

correlation $\mathscr{G}$ clearly coincides with $\langle S_x S_y \rangle$ as expressed, on the basis of high-temperature diagrams, in $\tanh(K_{\text{Ising}})$.

This is sufficient to conclude that the walk W has a bulk correlation exponent η equal to 1/4, as appropriate to $\langle S_x S_y \rangle$ for the critical Ising model.[37] From this, $\gamma = 14/11$ also follows. The γ derived here, as well as the previously determined ν, are fully consistent with accurate numerical extrapolations in ref. 27.

The point described above is expected to be multicritical, like the Θ'-point discussed in Section 2. At variance with the case of the Θ'-point model with uncorrelated vacancies, it is not possible to express in an explicit and local form the effective interactions caused by the correlated vacancies on the walk. However, we would expect the effective interactions to be of finite range except possibly when the vacancies are at Ising criticality and have themselves an infinite range. In any case, consistent with the fact that in the $n \to 0$ limit the full free energy content of the model (3.1) is given by the Ising part, the walk exponents at the multicritical point can be extracted from the same conformal grid, with $c = 1/2$, as for the critical Ising spin problem.[24]

Below we consider several surface critical regimes at this multicritical point.

We start from a special regime. Let us consider the case of type (a) walks. Equations (3.1)–(3.3) do not fully specify the boundary conditions. Walks of type (a) are not allowed to step on hexagons with a + sign. Since the border of the Ising model is assumed with open conditions, we can decide that only one factor of the type $(1 - \sigma_{j^*(l)})/2$ is present in Eq. (3.1) when l belongs to the boundary. With this choice, which makes the border accessible to the walk, one can easily see that the average radius of a ring with one point on the boundary would be given by expression (3.3), where Σ is made up of a collection of closed loops and by a number of self-avoiding paths with *both ends* on the boundary. The loops do not touch the border. Indeed, for a triangular Ising system with open boundary conditions these loops and this path are the possible lines separating the + and − islands.

In Fig. 8a we give a schematic representation of the contributions to the denominator of Eq. (3.3) in this case. In the numerator the diagrams are the same, and the ring radius appears as an extra factor multiplying the weight.

We did not succeed in determining the fractal dimension of such a ring. However, a simple modification of the interactions with the border makes this determination possible. Let us consider in Eq. (3.3) a step fugacity $K_l' = K_l \exp(+2L_c)$ for l belonging to the border. With this choice it is clear that, when $K_l = K_c = \exp(-2L_c)$, and $L = L_c$ in Eq. (3.3), the

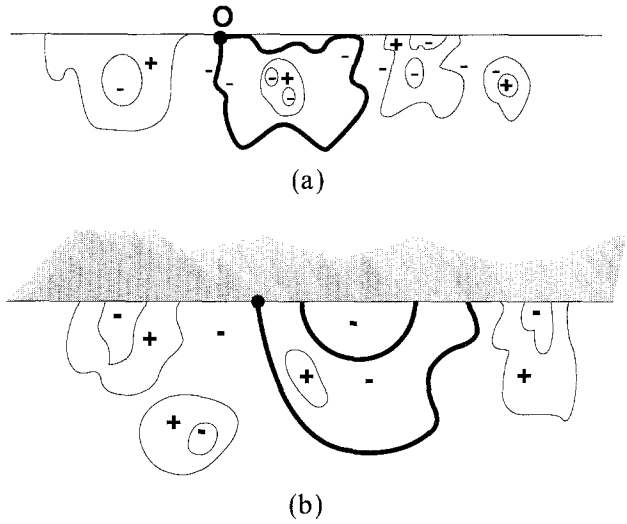

Fig. 8. (a) Representation of a typical contribution to the denominator of the quantity in Eq. (3.3). In this case the step fugacity on the boundary is $K_I = K$. (b) Diagrams for the case with $K_I = K\exp(2L_c)$ on the boundary. Steps of the ring belonging to the boundary are not represented by the heavy line and have an associated weight equal to unity.

weight associated with steps of the ring on the border in the configuration shown in Fig. 8b is just unity.

In this way the statistics of the ring becomes the same as that of hulls of Ising clusters with at least one hexagon on the border. But the geometry of critical Ising clusters at an open boundary is known.[38] The fractal dimension of their intersection with the boundary is 5/6, whereas the overall dimension of the hull is 11/8, as pointed out above. This gives the key to establishing that the ring in the situation just considered is in a special regime. Indeed, special regimes are characterized by

$$\langle N_s \rangle \sim (K_c - K)^{-\phi_s} \qquad \text{for} \quad K \to K_C^- \tag{3.5}$$

with $0 < \phi_s < 1$. In our case, taking into account that $(K_c - K) \sim 1/\langle N \rangle$, we have $\langle N_s \rangle \sim \langle N \rangle^{(5/6)(8/11)}$, and conclude that $\phi_s = 20/33$. We notice that the special regime just identified is one in which a sort of attraction of the ring by the boundary operates; this attraction is a consequence of the modification $K \to K\exp(2L_c)$ for hexagonal edges on the boundary.

To get η_s and γ_1 we need to consider the correlation function (3.4) for **x** and **y** in the neighborhood of the border. The typical contributions to the numerator of Eq. (3.4) are sketched in Figs. 9a and 9b.

The diagrams are the high-temperature ones for a hexagonal-lattice Ising-model correlation $G_1 = \langle S_{\mathbf{x}} S_{\mathbf{y}} \rangle$ in the presence of, e.g., plus bound-

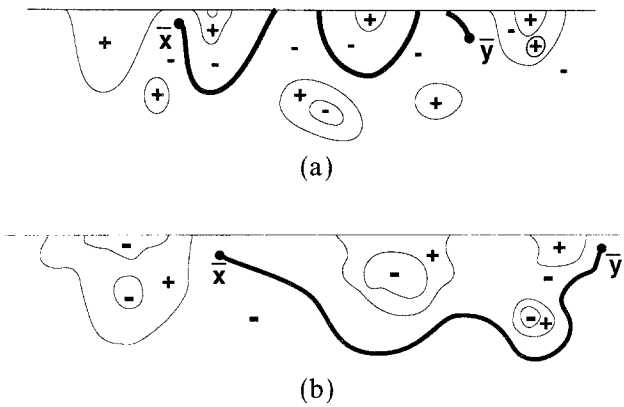

Fig. 9. (a) Diagram for the correlation $\mathscr{G}_1$ of type (a) walk for the case in which the SAW connecting **x** to **y** steps on the border. As in Fig. 8b, the choice $K_l = K\exp(2L_c)$ on the boundary gives an effective weight 1 to steps of the walk on the surface. (b) Diagram for $\mathscr{G}_1$, in case the type (a) SAW from **x** to **y** does not step on the boundary.

ary conditions. Indeed, consider an Ising model with border + as in Fig. 10a.

For such a model, diagrams contributing to the numerator of G_1 in a high-temperature diagrammatic expansion in $\tanh(K_{\text{Ising}}) = \exp(-2L_c)$ can be separated into three different groups. In the first one we consider those sketched in the Fig. 10b, which are characterized by the presence of a self-avoiding path joining **x** to **y**, and not touching the border.

In the second and third groups, we can put those sketched in Figs. 10c and 10d, respectively.

The diagrams in both Figs. 10c and 10d have paths connecting **x** and **y** to the boundary. The difference between the two groups amounts to the fact that in Fig. 10c there is no path with both ends on the boundary enclosing simultaneously **x** and **y**. In Fig. 10d there is one such path. The group of diagrams represented by Fig. 10d is that in which there is at least one of such enclosing path.

Diagrams in Fig. 10b for G_1 are also found, with identical weight, in $\mathscr{G}_1$. The same holds for diagrams in Fig. 10c. As a matter of fact all these diagrams appear in both G_1 and $\mathscr{G}_1$ with the same multiplicity equal to 1. In contrast, the diagrams sketched in Fig. 10d contribute with different multiplicities to G_1 and $\mathscr{G}_1$. Indeed, while they enter with multiplicity 1 in G_1, in the case of $\mathscr{G}_1$ there are always two different choices for the walk joining **x** to **y** leading to the same overall diagram. Thus, this multiplicity 2 is due to the fact that in $\mathscr{G}_1$ we distinguish between walk and hulls, even if we fix their weights as equal.

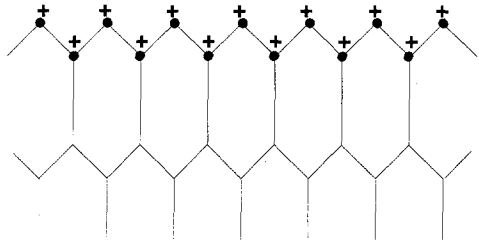

(a)

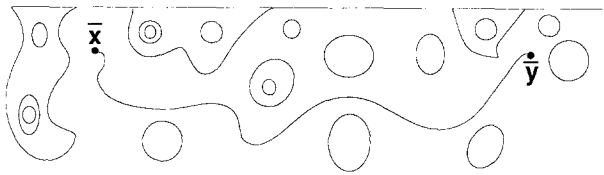

(b)

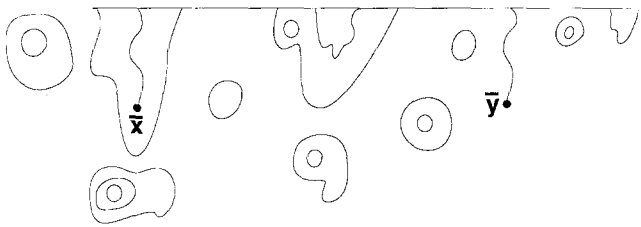

(c)

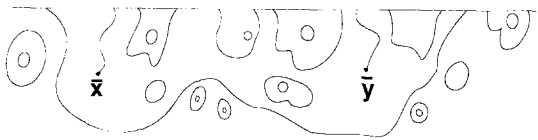

(d)

Fig. 10. (a) Boundary condition for an Ising problem on a hexagonal lattice, whose high-temperature expansion for $\langle S_x S_y \rangle$ leads to the same diagrams as in Figs. 9a and 9b. (b, c, d) Three types of diagrams for $G_1 = \langle S_x S_y \rangle$ of the Ising model with boundary condition as in panel (a). Each step has a weight $\tanh(K_{\text{Ising}}) = \exp(-2L_c)$.

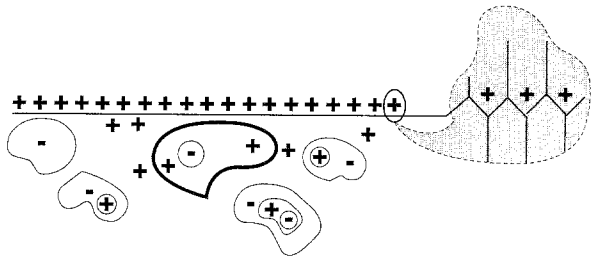

Fig. 11. Type (b) ring with + boundary condition on the dual triangular lattice. With these conditions, the Hamiltonian in Eq. (3.1) must contain terms of interaction between the boundary fluctuating hexagons and the fixed ones.

We expect $G_1 = \langle S_{\mathbf{x}} S_{\mathbf{y}} \rangle$ to factorize into the nonzero product $\langle S_{\mathbf{x}} \rangle \langle S_{\mathbf{y}} \rangle$ for $|\mathbf{x} - \mathbf{y}| \to \infty$ ($\mathbf{x}$ and $\mathbf{y}$ at finite distance from the boundary). Indeed, although the Ising system is at criticality, and thus has no long-range order in the bulk, the spins at $\mathbf{x}$ and $\mathbf{y}$ feel the action of the + boundary conditions. Since in $\mathscr{G}_1$ we have the same diagrams as in G_1, with multiplicities which are either the same or double, with their contribution positive, we conclude also that $\mathscr{G}_1$ does not go to zero for $|\mathbf{x} - \mathbf{y}| \to \infty$. This means that at the special point of our walks $\eta_s = 0$, thus $\gamma_1 = 15/11$.[7]

This value of γ_1 has been also checked numerically using an efficient Monte Carlo method already successfully applied to interacting polymer model.[4] Such an analysis gives $\gamma_1 = 1.4 \pm 0.1$, in good agreement with the theoretical prediction.

Up to now we have considered open boundary conditions for the spins on the dual, triangular lattice. In order to learn something about possible ordinary regimes of surface criticality, let us consider below type (b) walks, with the + boundary condition for the triangular Ising problem, as sketched in Fig. 11.

Clearly in this case ring statistics will coincide with hull statistics if the step fugacity is put *everywhere* equal to $K_I = \exp(-2L_c)$, also for the bonds on the boundary. Unfortunately, the fractal dimension of a hull on the boundary in the presence of closed, + conditions in the Ising model is not known exactly; it is very plausible, however, that, while the global hull fractal dimension remains 11/8, the dimension of its intersection with the

[7] In ref. 16, on the basis of a purely numerical investigation, we reported $\gamma_1 = 0.99 \pm 0.04$ at the special point, which suggested a value $\gamma_1 = 1$, as now found (see below) for one of the ordinary regimes. However, the numerical investigation there, being not based on a detailed analysis of the effects of all possible boundary conditions, like the present one, was fairly inaccurate, and its results partly spurious. E.g., no attempt was made there to distinguish between different ordinary regimes, as we do here.

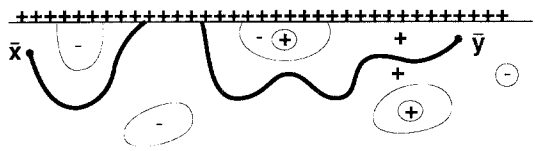

Fig. 12. Sketch of a typical configuration occurring in the numerator of $\mathscr{G}_1$ for type (b) walks in the presence of + boundary conditions for the Ising model.

boundary is equal to zero, even if the hull remains grafted at some point on the boundary. This is because the + condition acts as a sort of repulsion from the boundary for hexagons with spin -1. We thus expect that now the type (b) walk will be in an ordinary type of critical regime. For such a case it still makes sense to discuss the η_s and γ_1 exponents.

It is easy to realize that the diagrams contributing to the numerator of $\mathscr{G}_1$ in the last case considered above are those of the type shown in Fig. 12.

This, by duality, makes $\mathscr{G}_1$ equal to the correlation function of a hexagonal Ising model with open boundary conditions at the critical point, $\tanh(K_{\text{Ising}}) = \exp(-2L_c)$. This function is know to decay to zero as[39]

$$G_1(\mathbf{x}, \mathbf{y}) = \langle S_{\mathbf{x}} S_{\mathbf{y}} \rangle \sim |\mathbf{x} - \mathbf{y}|^{-1}$$

Thus $\eta_s = 1$ and $\gamma_1 = 1$. This last prediction, together with the claim that the fractal dimension of the ring on the boundary should be zero, have been tested numerically. We obtained $\gamma_1 = 1.00 \pm 0.05$ and $\langle N_s \rangle \sim (K_c - K)^{0.03 \pm 0.05}$.

Finally, it is interesting to consider the case of a walk of type (a) with the same + boundary conditions of the previous case. Since the walk can develop only on $-$ hexagons, the repulsion of the boundary is even stronger, and we anticipate ordinary behavior again. The discussion of $\mathscr{G}_1$ is easy also in this case; while the diagrams contributing to its denominator

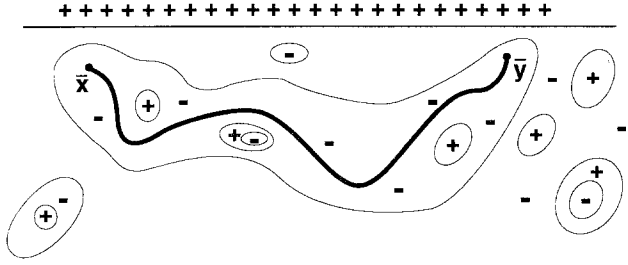

Fig. 13. Diagrams of the numerator of $\mathscr{G}_1$ for type (a) walks in the presence of + boundary conditions.

are exactly the same as in the previous case, now clearly the numerator has contributions of the type sketched in Fig. 13.

With a reasoning similar to that made for the ordinary Θ'-point, we conclude that this time the leading asymptotic behavior of $\mathscr{G}_1$ should be given by a watermelon function with $L=3$ for the *critical* Ising model. It turns out that for this function $x^s_{L=3}=7/2$; thus $\eta_s=7$ in this case while $\gamma_1=-13/11$.

This finding is rather interesting because it implies that for walks on correlated vacancies more than one ordinary surface regime can be realized, due to the effect of different boundary conditions imposed on the vacancies and on the walks.

Unfortunately the last prediction for γ_1 is also a very hard one to verify numerically, due to the difficulty in sampling walk configurations of the type sketched in Fig. 13. These configurations require the presence of a very big $-$ cluster enclosing and connecting both **x** and **y**, and this is rather difficult to sample in the presence of the $+$ boundary conditions.

It is worth noticing that all the above results for surface exponents with correlated vacancies are consistent with the assumption of a central charge $c=1/2$, and thus are further confirmation of this value.

4. SURFACE CROSSOVER EXPONENT OF NONINTERACTING SAW

The results obtained in the previous sections are a clear illustration of how powerful the vacancy approach can be for describing surface critical phenomena of interacting SAW. One of the advantages of this approach is that, as in the bulk case, vacancies provide substantial extra geometrical and physical insight into critical exponents, especially the crossover one, which is related to cluster fractal dimensions in all cases. One may wonder whether comparable insight could be provided by the vacancy approach in other, even relatively less complex cases.

When the SAW is not self-interacting, but only attracted by the boundary, it is by now established, both numerically and on the basis of conformal invariance results, that $\phi_s=1/2$ at the special transition.[15,21]

Below we reinterpret this result in terms of the geometry of percolation clusters.

Consider percolation on a semi-infinite square lattice. Elementary squares can be occupied or vacant with probability p or $1-p$, respectively.

A cluster is considered connected if one can join any couple of its squares by a path of nearest-neighbor squares of the cluster itself: squares sharing only one corner are thus considered as disconnected.

It was first noticed in ref. 40 that different definitions of the external perimeter of connected clusters can lead to different fractal dimensions. In general one defines the hull as constituted by the set of all edges of occupied squares separating the cluster from "external" vacant squares. In one case one includes in this set all the vacant squares that can be joined to the boundary at infinity through nearest-neighbor or next-nearest-neighbor vacant squares with connections. Alternatively, one can restrict the last condition by considering connections through nearest-neighbor vacant squares only. For a cluster like that in Fig. 14, the above two definitions clearly give different hulls. According to the first one, the hull includes the external perimeter plus the internal contour including vacant squares (dotted region) connected to infinity by paths through the point A. In this way the hull has configurations of the type appropriate to the static silhouette of a one-tolerant closed trail, i.e., a lattice walk which is allowed to self-intersect, but not to step more than once on a given lattice edge.

According to the latter definition, on the other hand, contours of regions like the dotted one in Fig. 14 are not included. Thus self-intersections are fully excluded and the hull configurations are those of a self-avoiding ring.

In the bulk a numerical investigation[40] showed that only the definition of hull implying one-tolerant trail silhouette shapes conforms to the expected hull fractal dimension equal to 7/4.[28] The second definition, restricting the hull configurations to those of a self-avoiding ring, implies a hull fractal dimension which, within the numerical accuracy, coincides with that of noninteracting SAW (i.e., 4/3).

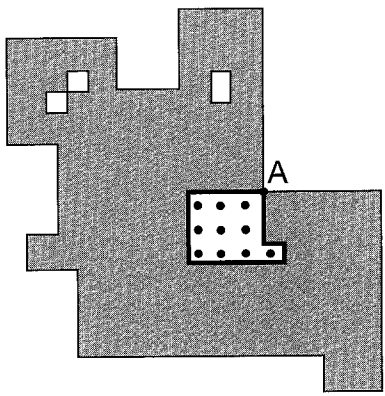

Fig. 14. Percolation cluster on a square lattice. The shaded region corresponds to sites of the cluster. The boundary of the dotted region might or might not be included in the hull definition.

In the spirit of the vacancy approach we can consider the statistics of this last type of hull as identical to that of an interacting self-avoiding ring. For a given configuration, the Boltzmann factor due to vacancy-mediated interactions can be written as

$$p^{N_1}(1-p)^{N_2} \tag{4.1}$$

where N_1 and N_2 are the total numbers of squares respectively internal and external to the ring, whose occupation status has to be specified in order to identity the given ring with a hull configuration. No matter how complicated the counting rules for N_1 and N_2 actually are, the important fact here is that these rules are clearly consistent with assuming a set of local interactions for the ring. What we deduce from the above numerical investigations is that, at $p = p_c = 0.592746...$,[41] the square lattice site percolation threshold, and with a ring step fugacity $K_c = 1$, the interacting SAR must be critical, with $\nu = 3/4$. This means that the vacancy-induced interactions are not attractive enough to induce Θ or collapsed bulk behavior.

Considering the same SAR problem at a linear boundary in semi-infinite geometry, we understand immediately that the boundary will exert a sort of attractive interaction on the ring. Most interesting for us here is the fact that, for hulls defined according to the two alternatives specified above, the intersection with the boundary has a weight, as a function of p, which is the same if the intersection is the same, in spite of the fact that the global hull profile is defined very differently in the two cases. Indeed, enclosures like the dotted one in Fig. 14 can obviously never reach an edge on the boundary of the lattice. So, whether such enclosures are counted or not in evaluating the total hull length, the statistics of the intersection of the hull with the boundary is left unaffected. This means that if we fix $p = p_c$ ad $K = K_c = 1$ as step fugacity for our SAR, its intersection with the boundary must have the same fractal dimension as the intersection of the critical percolation hull, defined in the *proper* sense (i.e., with enclosures). This dimension, as we discussed in Section 2, is equal to 2/3.[25] Our self-avoiding ring at $p = p_c$ and $K = K_c = 1$ has thus an average number of steps on the boundary $\langle N_s \rangle$ growing as $R^{2/3}$ if R is the average radius of gyration with respect to the center of mass. Since, as we said above, one should have

$$R \sim (K_c - K)^{-3/4}, \qquad K \to K_c^- \tag{4.2}$$

we conclude

$$\langle N_s \rangle \sim (K_c - K)^{-1/2}, \qquad K \to K_c^- \tag{4.3}$$

So, $p = p_c$ and $K = K_c = 1$ locates the special transition point for our ring on the boundary. Since the ν exponent for the ring is 3/4, this point must be in the same universality class as the special transition of noninteracting SAW. For such a transition the surface crossover exponent is thus $\phi_s = 1/2$, as recently established on the basis of conformal invariance considerations,[21] in full agreement with the numerical results.[20,15]

5. CONCLUSIONS

In the present work we have shown how the idea of vancancy-mediated interactions can be exploited to give an exact and complete description of the surface criticality of interacting polymer models in $d = 2$ when the bulk behavior is simultaneously multicritical. The best known case is that of a SAW at the bulk Θ transition, which can simultaneously undergo an adsorption transition upon increasing the attractive interaction with the boundary. We showed that a careful discussion of boundary conditions for the so-called Θ'-point model with uncorrelated vacancies allows identification and exact characterization of the ordinary and special Θ'-regimes. Even if the exact results obtained here for the exponents strictly refer to a specific model of polymer collapse and adsorption, a very recent extensive series of investigations of a more standard model[18] seems to support rather nicely universality of surface and bulk Θ behavior in $d = 2$.[8] The results obtained here for γ_{1o} and γ_{1sp} eliminate, in our opinion, the most serious source of doubts about Θ-universality. Indeed, the numerical estimates of these exponents also for other models[7,15] in the literature do not show major discrepancies with our Θ'-model results. This was not of course the case with the previous conjecture, $\gamma_{1o} = 8/7$,[3] which is revealed here to be incorrect.

In spite of the possibility that numerical problems could still hinder progress on the general issue of verifying Θ-point universality, the fact that now a full set of bulk and surface exponents has been determined in a given model is certainly a useful step forward, in our opinion.

Correlated vacancies were already known to be able to produce new bulk multicritical phenomena for interacting SAW in $d = 2$.[27] Here we

[8] At variance with the conclusions of ref. 18, the authors of a recent Monte Carlo study[19] of standard Θ-point models interpret discrepancies of their results from Θ'-point exact exponents as indications of nonuniversality. However, the numerical verification of such universality should be made, in our opinion, with a most generous attitude as far as confidence limits of the results are concerned. A further important consistency test of such methods should be their application to cases without interactions, specifically to the study of the special transition of SAW.

have shown that the vacancy approach to surface critical phenomena can lead also in this case to interesting new exact results for critical exponents. A rather remarkable fact we demonstrated is also the possibility of more than one ordinary regime for a SAW at the new bulk multicritical point. Indeed when surface interactions are mediated by correlated vacancies, different boundary conditions imposed on these vacancies can lead to different universality classes for ordinary surface behavior. This somewhat unexpected feature is quite intriguing and ought to be further investigated.

A final result we presented here is a new derivation, based on the geometry of percolation vacancies, of the value $\phi_s = 1/2$ for the surface crossover exponent of noninteracting SAW. This derivation shows that the idea of vacancies can be extended to cases in which the bulk behavior is not multicritical. In addition, the new interpretation of ϕ_s shows that the connection between SAW problems and percolation is deeper and wider than already shown by earlier[3,27] and present developments concerning the Θ'-point and related issues.

ACKNOWLEDGMENT

F.S. would like to acknowledge support from the European Community through the SCIENCE program. A.L.S. acknowledges partial support from INFM.

REFERENCES

1. K. Binder, in *Phase Transitions and Critical Phenomena*, Vol. 8, C. Domb and J. L. Lebowitz, eds. (Academic Press, 1983).
2. A. Coniglio, N. Jan, I. Maijd, and H. E. Stanley, *Phys. Rev. B* **35**:3617 (1987).
3. B. Duplantier and H. Saleur, *Phys. Rev. Lett.* **59**:539 (1987).
4. F. Seno and A. L. Stella, *J. Phys.* (Paris) **49**:739 (1988).
5. P. H. Poole, A. Coniglio, N. Jan, and H. E. Stanley, *Phys. Rev. B* **39**:495 (1989).
6. B. Duplantier and H. Saleur, *Phys. Rev. Lett.* **60**:1204 (1988).
7. F. Seno and A. L. Stella, *Europhys. Lett.* **7**:605 (1988).
8. F. Seno, A. L. Stella, and C. Vanderzande, *Phys. Rev. Lett.* **61**:1520 (1988).
9. B. Duplantier and H. Saleur, *Phys. Rev. Lett.* **61**:1521 (1988).
10. P. H. Poole, A. Coniglio, N. Jan, and H. E. Stanley, *Phys. Rev. B* **39**:495 (1989).
11. H. Meirovitch and H. A. Lim, *Phys. Rev. Lett.* **62**:2640 (1989).
12. B. Duplantier and H. Saleur, *Phys. Rev. Lett.* **62**:2641 (1989).
13. I. S. Chang, H. Meirovitch, and Y. Shapir, *Phys. Rev. A* **41**:1808 (1990).
14. D. Maes and C. Vanderzande, *Phys. Rev. A* **41**:3074 (1990).
15. A. R. Veal, J. M. Yeomans, and G. Jug, *J. Phys. A* **24**:827 (1991).
16. C. Vanderzande, A. L. Stella, and F. Seno, *Phys. Rev. Lett.* **67**:2757 (1991).
17. S. O. Warnaar, M. T. Batchelor, and B. Nienhuis, *J. Phys. A* **25**:3077 (1992).
18. D. P. Foster, E. Orlandini, and M. C. Tesi, *J. Phys. A* **25**:1211 (1992).
19. I. Chang and H. Meirovitch, *Phys. Rev. Lett.* **69**:2232 (1992).
20. I. Guim and T. W. Burkhardt, *J. Phys. A* **22**:1131 (1989).

21. T. W. Burkhardt, E. Eisenriegler, and I. Guim, *Nucl. Phys.* **316**:559 (1989).
22. P. Flory, *Principles of Polymer Chemistry* (Cornell University Press, Ithaca, New York, 1971).
23. P. G. de Gennes, *Scaling Concepts in Polymer Physics* (Cornell University Press, Ithaca, New York, 1979).
24. J. Cardy, in *Phase Transitions and Critical Phenomena*, Vol. 11, C. Domb and J. L. Lebowitz, eds. (Academic Press, 1987).
25. J. L. Cardy, *Nucl. Phys. B* **240**:514 (1984).
26. B. Duplantier and H. Saleur, *Phys. Rev. Lett.* **57**:3179 (1986).
27. F. Seno, A. L. Stella, and C. Vanderzande, *Phys. Rev. Lett.* **65**:2897 (1990).
28. H. Saleur and B. Duplantier, *Phys. Rev. Lett.* **58**:2325 (1987).
29. C. Vanderzande, *J. Phys. A* **21**:833 (1988).
30. H. Saleur, *J. Phys. A* **19**:L807 (1986).
31. H. Saleur, *J. Phys. A* **20**:457 (1987).
32. B. Nienhuis, in *Phase Transitions and Critical Phenomena*, Vol. 11, C. Domb and J. L. Lebowitz, eds. (Academic Press, 1987).
33. B. Duplantier, *Phys. Rep.* **184**:229 (1989).
34. B. Duplantier, *J. Phys. A* **19**:L1009 (1986).
35. J. Groenewald and B. Nienhuis, in preparation.
36. A. L. Stella and C. Vanderzande, *Phys. Rev. Lett.* **62**:1067 (1989).
37. B. Kaufman and L. Onsager, *Phys. Rev.* **76**:1244 (1949).
38. C. Vanderzande and A. L. Stella, *J. Phys. A* **22**:L445 (1989).
39. B. M. McCoy and T. T. Wu, *Phys. Rev.* **162**:436 (1967).
40. T. Grossmann and A. Aharony, *J. Phys. A* **19**:1745 (1986).
41. R. M. Ziff, *Phys. Rev. Lett.* **69**:2670 (1992).